

## Supporting information

### From Elementary to Advanced: Rational Designing Single Component Phosphorescence Organogels for Anti-Counterfeiting Applications

Huamiao Lin,<sup>a,b</sup> Yi Shi,<sup>a</sup> Yan Li,<sup>a</sup> Shuzhan Chen,<sup>a</sup> Wei Wang,<sup>a</sup> Peng Geng,<sup>\*,a,b</sup> Jiaying Yan<sup>a,b</sup> and Shuzhang Xiao<sup>\*,a,b</sup>

<sup>a</sup> Key Laboratory of Inorganic Nonmetallic Crystalline and Energy Conversion Materials, College of Materials and Chemical Engineering, China Three Gorges University, Yichang, Hubei 443002, China

<sup>b</sup> Hubei Three Gorges Laboratory, Yichang, Hubei 443007, China

#### 1. Methods and Measurements

##### (1) Measurements

All starting materials were obtained from commercial supplies and used as received. <sup>1</sup>H NMR spectra were recorded on a Bruker 400 NMR spectrometer. Chemical shifts were reported in parts per million (ppm) using tetramethylsilane (TMS) as a reference and CDCl<sub>3</sub> as the solvent. HRMS data were recorded on an Applied Biosystems Voyager-DE STR mass spectrometer. UV-vis spectra were measured using a Shimadzu UV-2600 spectrometer, and fluorescence spectra using a Hitachi F-4600 spectrometer. Fluorescence quantum yields and lifetime measurements for solid powders and crystals were performed on an Edinburgh FS5 luminescence spectrometer, using a 375 nm excitation source. Phosphorescence lifetimes were measured using an Edinburgh FS5 spectrometer equipped with a micro flash-lamp (MCS diode). SEM images of the xerogels were obtained using an SSX-550 (Shimadzu). Optical microscopy images were captured using a LEICA DMi8 fluorescence microscope. XRD diagrams were obtained using a D8 ADVANCE (Bruker). Rheological measurements were carried out on freshly prepared gels using a Malvern Bohlin GeminiHRnano controlled stress rheometer. The single-crystal X-ray diffraction data was collected on a Rigaku XtaLAB PRO single-crystal X-ray

diffractometer equipped with a graphite monochromated Cu K $\alpha$  radiation ( $\lambda = 1.54 \text{ \AA}$ ) at 298 K.

## **(2) Molecular dynamics simulation**

MD simulations involved placing 5 gelator molecules in a periodic cubic box with solvent molecules to achieve a 5.0% w/v concentration. This concentration was also used to determine gelation performance experimentally. A 50 ns trajectory with a 0.5 fs timestep was recorded using the Amber99sb-ildn force field. Parameters were retrieved from the Sobtop and Multiwfn service. Before production simulations, energy minimization and temperature/pressure equilibration were performed to prevent steric clashes and ensure proper NPT-ensemble equilibration. The simulations utilized the V-rescale thermostat and Parrinello-Rahman barostat, maintaining a temperature of 298K and a pressure of 1.0 bar. All molecules were randomly placed in the simulation box using Packmol, with gelator molecules dispersed separately in the solvent. Simulations were run using Gromacs software version 2018.8<sup>1</sup>. Descriptors were calculated as time averages over the 50 ns simulation period, following methods from a previous report<sup>2</sup>. Details are provided as follows:

### **(I) Calculating SASA, R<sub>max</sub> and V**

Fully extended molecules are saved as a PDB file with all main chain dihedral angles set to 180°, without additional structure optimization. R<sub>max</sub> measures the distance between the furthest atoms in a fully extended conformation. The SASA for the fully extended conformation was calculated using GROMACS' gmx sasa tool. To generate the index file (index.ndx), the PDB file of the extended molecule was processed with the GROMACS command: **gmx make\_ndx -f 180.pdb -o index.ndx**. The SASA of the extended molecule was calculated using the command: **gmx sasa -f 180.pdb -s 180.pdb -n index.ndx -o sasa.xvg**. During the SASA calculation, the software prompts for a group selection, where the entire system is chosen. Gelator molecular volume (V) is determined using the Marching Tetrahedron (MT) algorithm in Multiwfn software.

### **(II) Calculating rSASA**

$$rSASA = \frac{\overline{SASA}}{SASA_{\max}}$$

$SASA_{\max}$  is calculated by multiplying the SASA of the fully extended gelator molecules by their total number in the simulation, which is five. To calculate the average SASA ( $\overline{SASA}$ ), a trajectory file (.xtc) and a GROMACS structure file (prod.gro) are needed, with solvent and gelator molecules labeled as SOL and GEL, respectively, to exclusively track gelator molecules. The index file (.ndx) is created using the command: **gmx make\_ndx -f prod.gro -o indexprod.ndx**. Subsequently, the SASA changes during the simulation are calculated with: **gmx sasa -f prod.xtc -s prod.gro -n indexprod.ndx -surface GEL -o sasaprod.xvg**. The mean SASA is calculated using the sasaprod.xvg file with the command: **gmx analyze -f sasaprod.xvg**.

### (III) Calculating rH


$$rH = \frac{\overline{R}}{R_{\max}}$$

To calculate the average distance  $\overline{R}$ , create an index file (indexrH.ndx) listing the furthest apart atoms of each gelator molecule, for instance: **[gelator1] "index1 index2"** and **[gelator2] "index1 index2"**. The change in distance between these atoms during the simulation is calculated using the GROMACS command: **gmx distance -f prod.xtc -s prod.gro -n indexrH.ndx -oall rH.xvg**. During the calculation, GROMACS prompts for the selection of groups to calculate distances; all groups are selected. The rH.xvg file is then analyzed using the gmx analyze command to calculate the average distance  $\overline{R}$ .

### (IV) Calculating $F$

$$F = \frac{\overline{R_g}}{R_h}$$

$$\overline{R_g} = \sqrt{\frac{\sum_{i=1}^A m_i \times s_i^2}{\sum_{i=1}^A m_i}}$$



R<sub>h</sub>, representing a derived parameter, was calculated using the total number of gelator molecules (5) and their volume (V) during the simulation. The average radius of gyration,  $\bar{R}_g$ , is calculated with the GROMACS command: **gmx gyrate -f prod.xtc -s prod.tpr -o gyrate.xvg**. During the execution, GROMACS prompts for the selection of a group; the GEL group is selected to focus the calculation on gelator molecules. After obtaining the gyrate.xvg file, the gmx analyze command is used to calculate  $\bar{R}_g$ .

### **(3) TD-DFT calculation**

To gain insights into their excited triplet states, monomers and dimers were extracted from the final MD snapshot and analyzed using TD-DFT with the B3LYP functional and 6-31G(d,p) basis set. Similarly, spin-orbit coupling matrix elements (SOCMEs) were evaluated using ORCA software<sup>3</sup>. Molecular packing from the MD simulation results was analyzed using Mercury software to assess structural arrangement. The selected molecular cluster was calculated using the M06-2X/6-31G(d,p) level, including empirical dispersion correction (GD3). Subsequently, intermolecular interactions were analyzed using Multiwfn software<sup>4</sup>.

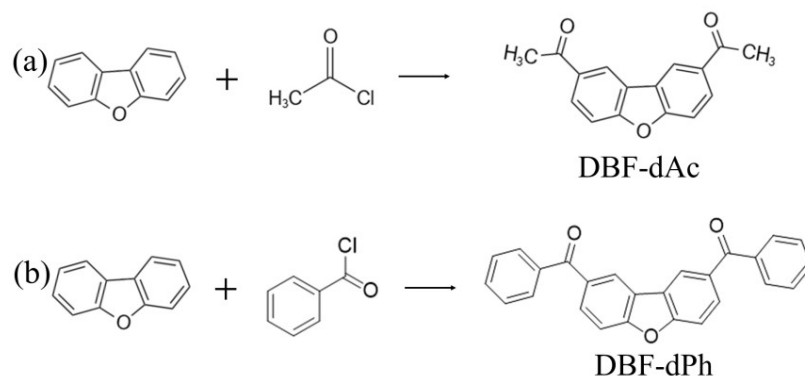
### **(4) Gelation test**

The gelator and solvent were placed in a septum-capped test tube and heated until the solid dissolved. Subsequently, the sample vial was cooled to room temperature either naturally or via sonication. Gelation was qualitatively deemed successful if the sample did not flow when the container was inverted at room temperature, using the inverse flow method. Xerogel samples were produced by freeze-drying to evaporate the solvent from the gel.

### **(5) Crystal cultivation**

Single crystals were cultivated in conventional organic solvents, such as THF, acetonitrile, THF and methanol. Finally, single crystal suitable for X-ray diffraction measurement was obtained for **DBF-dPh** in acetonitrile, and the CCDC number is 2350009.

## 2. Synthesis



**Scheme S1.** Synthetic routes of **DBF-dAc** (a) and **DBF-dPh** (b).

**DBF-dAc:** Under an atmosphere of nitrogen, chloroform (15 mL) was added to anhydrous  $\text{AlCl}_3$  (7.35 g, 55.29 mmol, 3.1 equiv). Subsequently, acetyl chloride (10.1 mL, 142.69 mmol, 8.0 equiv) was added dropwise under stirring. Then, dibenz[b,d]furan (3.00 g, 17.83 mmol, 1.0 equiv) in chloroform (50 mL) was slowly added to the reaction mixture, which was allowed to stir at room temperature overnight. Upon completion of the reaction, the mixture was quenched with dilute hydrochloric acid (HCl) and extracted three times with dichloromethane (DCM). The combined organic extracts were washed with water, dried over anhydrous sodium sulfate ( $\text{Na}_2\text{SO}_4$ ), and concentrated under vacuum. The crude product was purified by silica gel column chromatography to provide a yellow powder (60%).  $^1\text{H}$  NMR (400 MHz,  $\text{CDCl}_3$ ):  $\delta$  8.65 (d,  $J = 0.8$  Hz, 2H), 8.19 (m, 2H), 7.66 (d,  $J = 8.4$  Hz, 2H), 2.74 (s, 6H).  $^{13}\text{C}$  NMR (100 MHz,  $\text{CDCl}_3$ ):  $\delta$  197.00, 159.51, 133.10, 128.67, 124.12, 121.89, 111.99, 26.78. HRMS (ESI)  $m/z$ :  $[\text{M}+\text{H}]^+$  calcd for  $\text{C}_{26}\text{H}_{17}\text{O}_3$  253.0865, found 253.0876. The  $^1\text{H}$  NMR data matches the reference<sup>5</sup>.

**DBF-dPh:** Under an inert nitrogen atmosphere, chloroform (10 mL) was added to anhydrous  $\text{AlCl}_3$  (3.19 g, 24.0 mmol, 4.0 eq). This was followed by the slow

addition of benzoyl chloride (4.16 mL, 36.0 mmol, 6.0 eq). Subsequently, dibenz[b,d]furan (1.01 g, 6.0 mmol, 1.0 eq) dissolved in chloroform (20 mL) was gradually introduced into the previous reaction mixture and stirred at room temperature for 6 h. After completion of the reaction, the mixture was quenched with dilute hydrochloric acid (HCl) and extracted three times with dichloromethane (DCM). The combined organic extracts were washed with water, dried over anhydrous  $\text{Na}_2\text{SO}_4$ , and the crude product was concentrated under vacuum. The final product **DBF-dPh** was obtained through purification by column chromatography, providing a pale yellow solid (65%).  $^1\text{H}$  NMR (400 MHz,  $\text{CDCl}_3$ ):  $\delta$  8.45 (d,  $J = 1.2$  Hz, 2H), 8.06 (m, 2H), 7.85 (d,  $J = 7.2$  Hz, 4H), 7.72 (d,  $J = 8.8$  Hz, 2H), 7.65 (t,  $J = 7.4$  Hz, 2 H), 7.55 (t,  $J = 7.6$  Hz, 4H).  $^{13}\text{C}$  NMR (100 MHz,  $\text{CDCl}_3$ ):  $\delta$  195.95, 159.20, 137.83, 133.29, 132.45, 130.46, 129.99, 128.42, 123.86, 123.78, 111.87. HRMS (ESI)  $m/z$ :  $[\text{M}+\text{H}]^+$  calcd for  $\text{C}_{26}\text{H}_{17}\text{O}_3$  377.1178, found 377.1219.

### 3. Figures and Tables

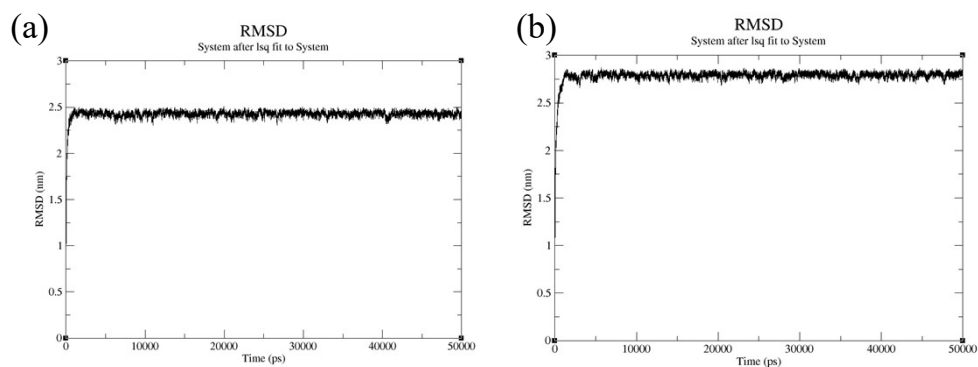


**Fig. S1** The root-mean-square deviation (RMSD) profile with respect to time in the self-assembly process of **DBF-dAc** (a) and **DBF-dPh** (b) in DMSO.

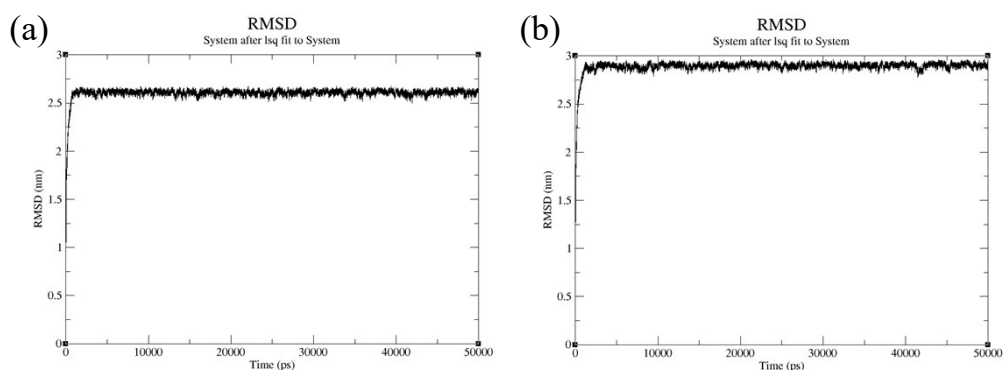


**Fig. S2** The root-mean-square deviation (RMSD) profile with respect to time in the self-assembly process of **DBF-dAc** (a) and **DBF-dPh** (b) in DMSO/H<sub>2</sub>O (2:1 v/v).

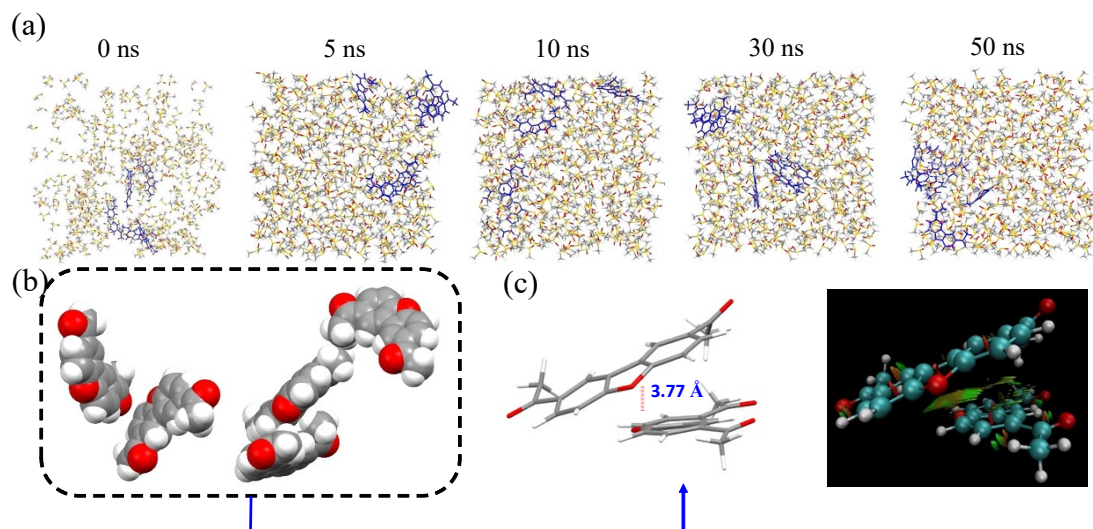


**Fig. S3** (a) Snapshots of MD simulation tracking the self-assembly of five **DBF-dAc** molecules in DMSO (**DBF-dAc** molecules are colored blue); (b) molecular stacking of the five **DBF-dAc** molecules from the final MD snapshot (50 ns); (c) intermolecular  $\pi$ - $\pi$  stacking of **DBF-dAc** as extracted from final MD snapshot ( $\pi$ - $\pi$  interaction is shown as green cloud).

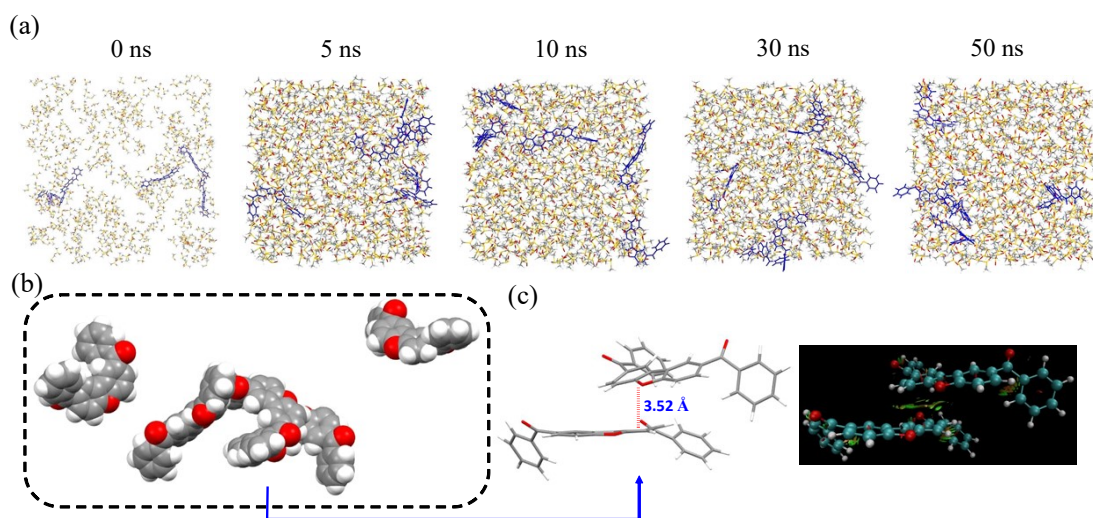


**Fig. S4** (A) Snapshots of MD simulation tracking the self-assembly of five **DBF-dPh** molecules in DMSO (**DBF-dPh** molecules are colored blue); (B) molecular stacking of the five **DBF-dPh** molecules from the final MD snapshot (50 ns); (C) intermolecular  $\pi$ - $\pi$  stacking of **DBF-dPh** as extracted from final MD snapshot ( $\pi$ - $\pi$  interaction is shown as green cloud).



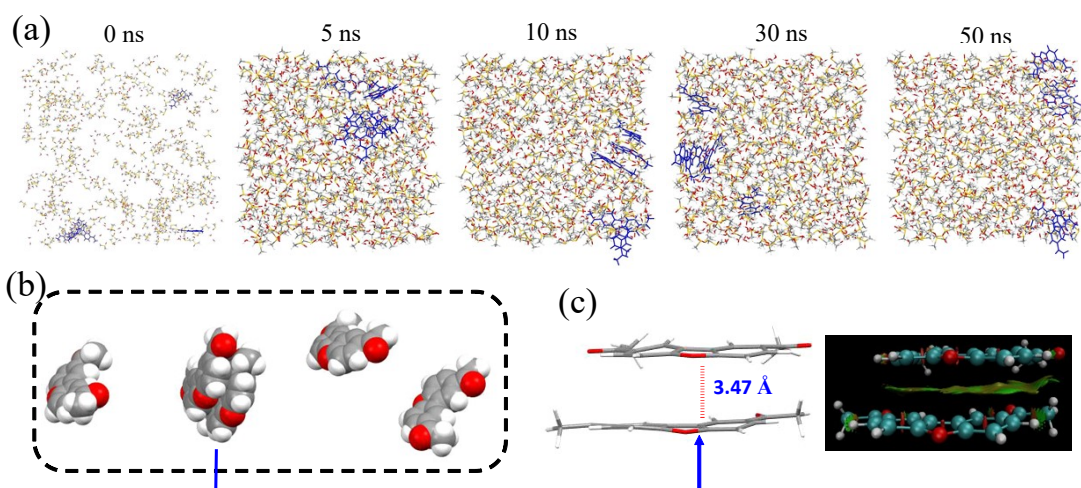


**Fig. S5** (a) Snapshots of MD simulation tracking the self-assembly of five **DBF-dAc** molecules in a mixture of DMSO and water (**DBF-dAc** molecules are colored blue); (b) molecular stacking of the five **DBF-dAc** molecules from the final MD snapshot (50 ns); (c) intermolecular  $\pi$ - $\pi$  stacking of **DBF-dAc** as extracted from final MD snapshot ( $\pi$ - $\pi$  interaction is shown as green cloud).

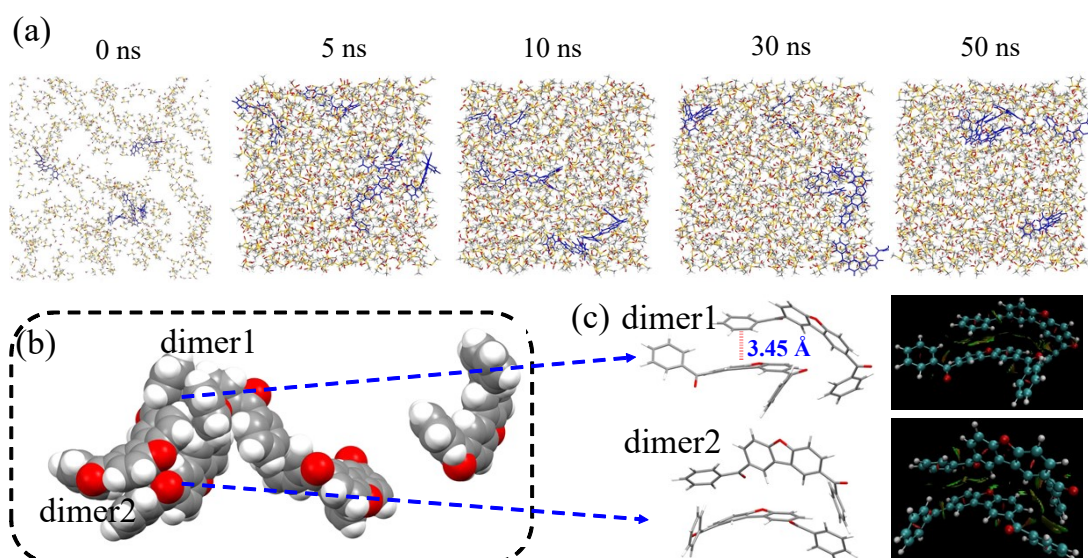


**Fig. S6** (A) Snapshots of MD simulation tracking the self-assembly of five **DBF-dPh** molecules in a mixture of DMSO and water (**DBF-dPh** molecules are colored blue); (B) molecular stacking of the five **DBF-dPh** molecules from the final MD snapshot (50 ns); (C) intermolecular  $\pi$ - $\pi$  stacking of **DBF-dPh** as extracted from final MD snapshot ( $\pi$ - $\pi$  interaction is shown as green cloud).



**Table S1.** Gelation test of synthesized compounds

Solvents	DBF-dAc	DBF-dPh
cyclohexane	In	In
Toluene	S	S
THF	S	S
acetonitrile	P	P
acetone	S	S
methanol	In	In
ethanol	In	In
DMSO	S	S
DMSO/H <sub>2</sub> O (2:1 v/v)	G (15 mg/mL)	G (20 mg/mL)

In: insoluble; P: precipitate; S: soluble; G: gel. CGC: critical gelation concentration (mg/mL)

Note: The numbers in brackets are CGC values; all the gels are formed by heating and sonication

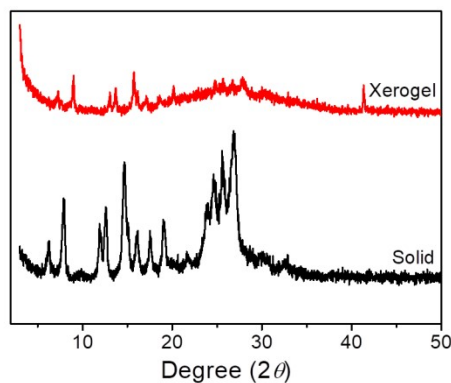


**Fig. S7** XRD pattern of **DBF-dAc** xerogel and solid from evaporation of eluent from column.

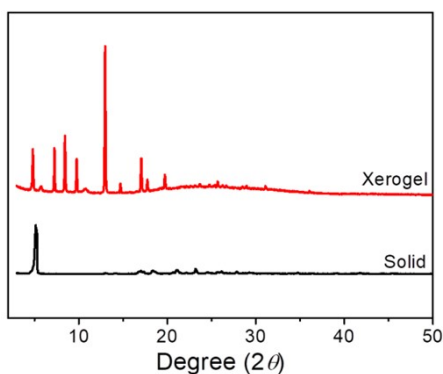


**Fig. S8** XRD pattern of **DBF-dPh** xerogel and solid from evaporation of eluent from column.

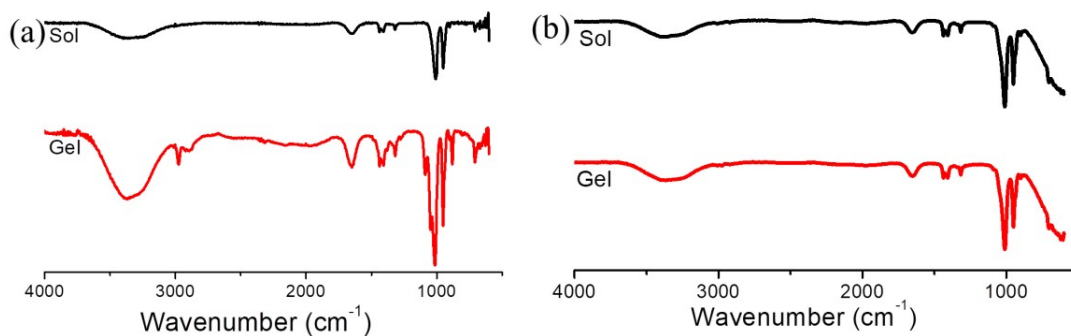


**Fig. S9** FTIR spectra of **DBF-dAc/DBF-dPh** in gel and sol states. (a) **DBF-dAc**; (b) **DBF-dPh**.

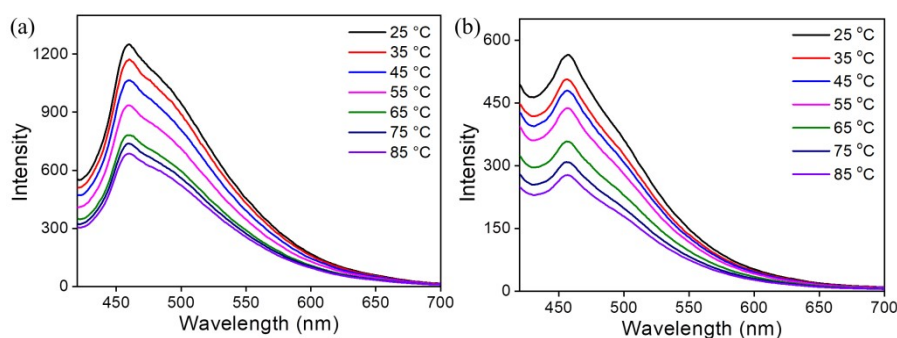


**Fig. S10** Fluorescence spectra of concentrated (10<sup>-2</sup> M, a) and dilute (10<sup>-5</sup> M, b) **DBF-dPh** solutions at different temperatures ( $\lambda_{\text{ex}}$ : 400 nm)

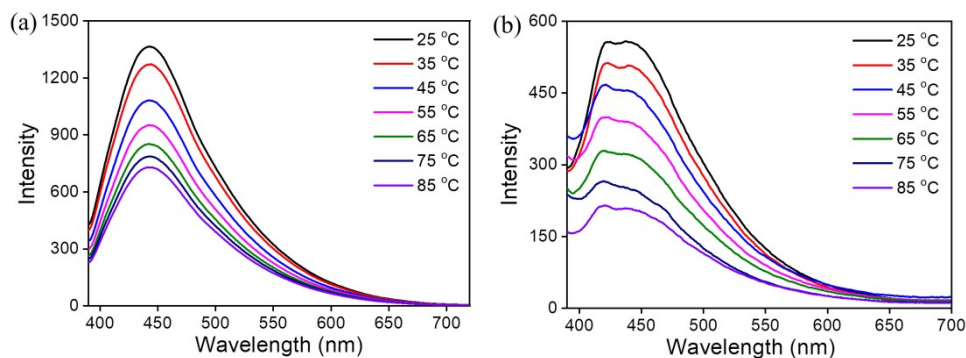


**Fig. S11** Fluorescence spectra of concentrated (10<sup>-2</sup> M, a) and dilute (10<sup>-5</sup> M, b) **DBF-dAc** solutions at different temperatures ( $\lambda_{\text{ex}}$ : 400 nm)

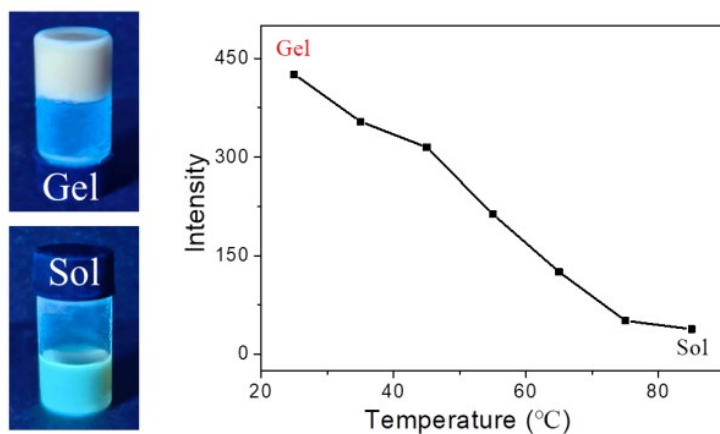


**Fig. S12** Steady-state photoluminescence intensity of **DBF-dAc** in DMSO/H<sub>2</sub>O during the sol-gel transition ( $\lambda_{\text{ex}}$ : 370 nm; concentration: 15 mg mL<sup>-1</sup>).

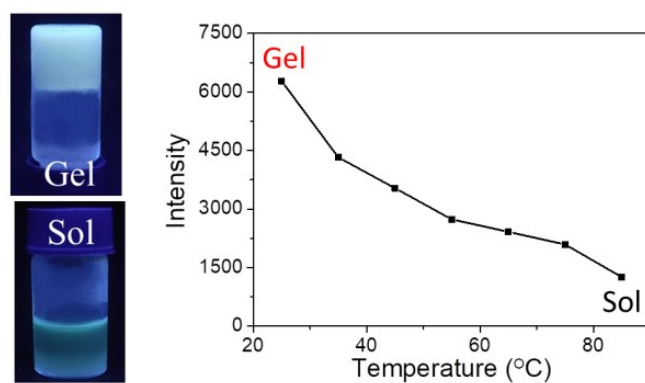


**Fig. S13** Steady-state photoluminescence intensity of **DBF-dPh** in DMSO/H<sub>2</sub>O during the sol-gel transition ( $\lambda_{\text{ex}}$ : 400 nm; concentration: 20 mg mL<sup>-1</sup>).

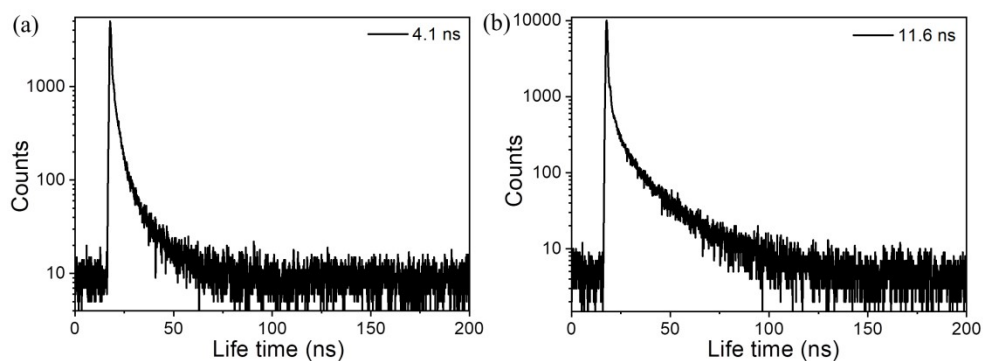


**Fig. S14** Fluorescence lifetimes of **DBF-dPh** gel (a) and **DBF-dAc** gel (b).

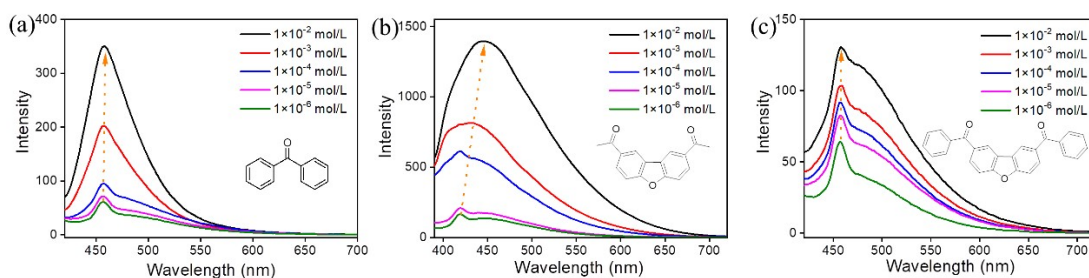


**Fig. S15** Concentration-dependent fluorescence spectra in DMSO. (a) benzophenone; (b) DBF-dAc; (c) DBF-dPh

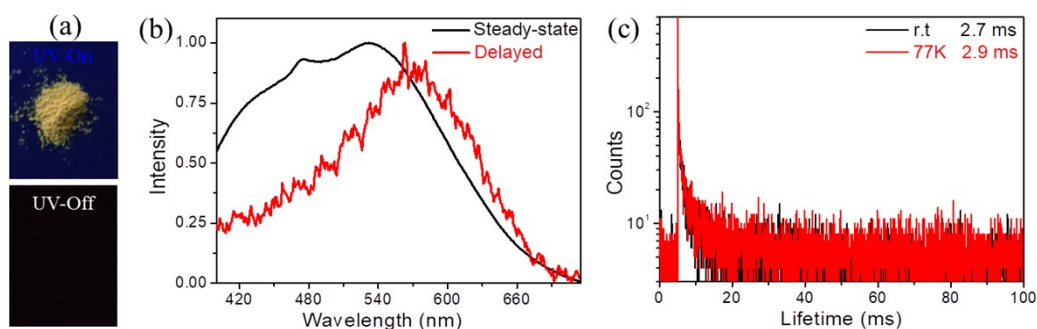


**Fig. S16** (a) Luminescent images; (b) steady-state and delayed spectra; (c) phosphorescence lifetime of **DBF-dAc** powder as obtained from column chromatography ( $\lambda_{\text{ex}}$ : 370 nm; delayed 1 ms).

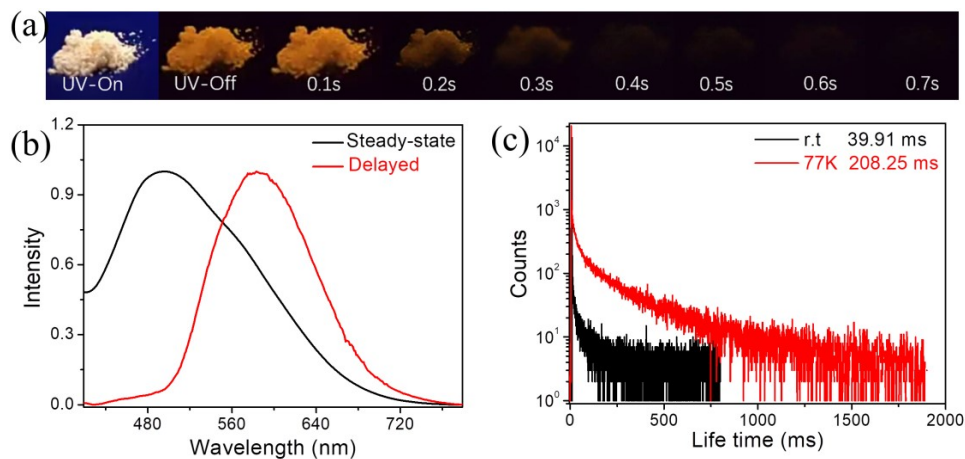


**Fig. S17** (a) Luminescent images; (b) steady-state and delayed spectra; (c) phosphorescence lifetime of **DBF-dPh** powder as obtained from column chromatography ( $\lambda_{\text{ex}}$ : 400 nm; delayed 1 ms).

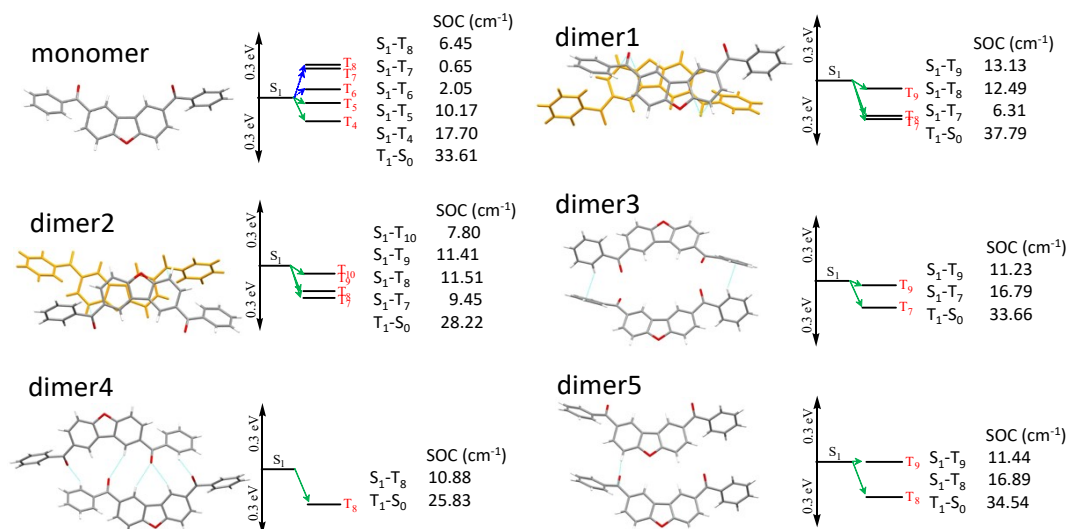


**Fig. S18** Monomer and dimers as extracted from the single crystal structure of **DBF-dPh** and their energy level diagrams calculated at B3LYP/6-31G(d,p).

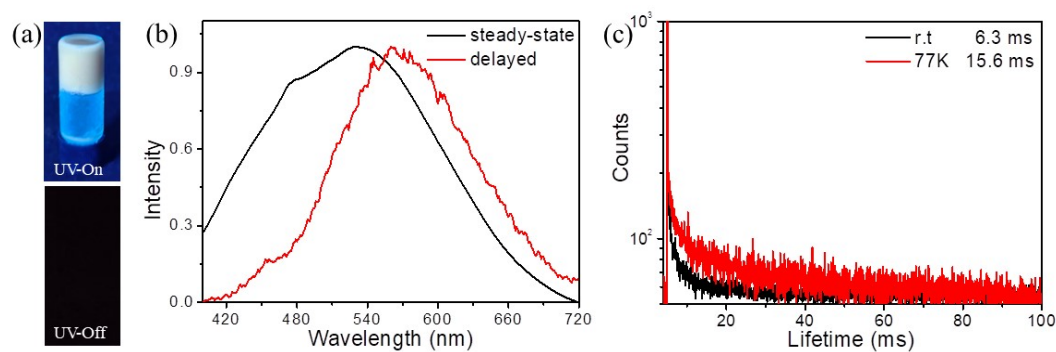


**Fig. S19** (a) Luminescent images; (b) steady-state and delayed spectra; (c) phosphorescence lifetime of **DBF-dAc** gel in DMSO/H<sub>2</sub>O ( $\lambda_{\text{ex}}$ : 370 nm; delayed 1 ms).

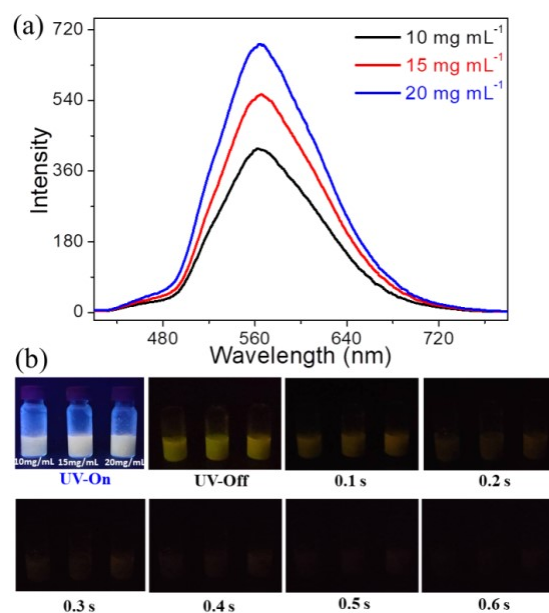


**Fig. S20** (a) Delayed emission spectra of **DBF-dPh** gel with different concentrations; (b) photoluminescence and afterglow images of **DBF-dPh** gel with different concentrations ( $\lambda_{\text{ex}}$ : 400 nm; delayed 1 ms).

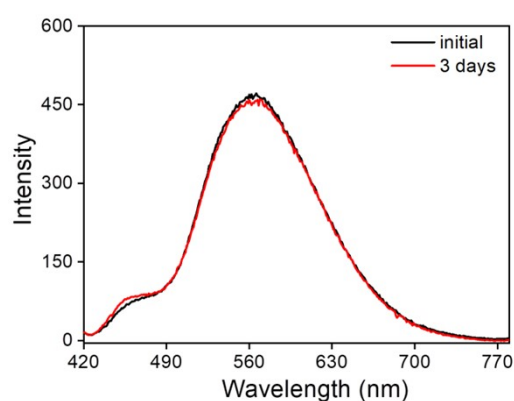


**Fig. S21** Delayed spectra of **DBF-dPh** gel in its initial state and after 3 days ( $\lambda_{\text{ex}}$ : 400 nm, delay: 1 ms).

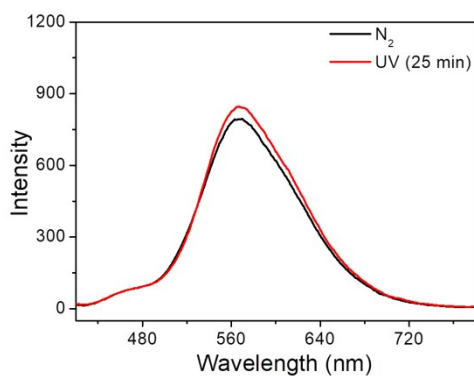


**Fig. S22** The phosphorescence spectra of **DBF-dPh** gel were performed before/after 25 min of UV irradiation in a nitrogen atmosphere ( $\lambda_{\text{ex}}$ : 400 nm; delayed 1 ms).

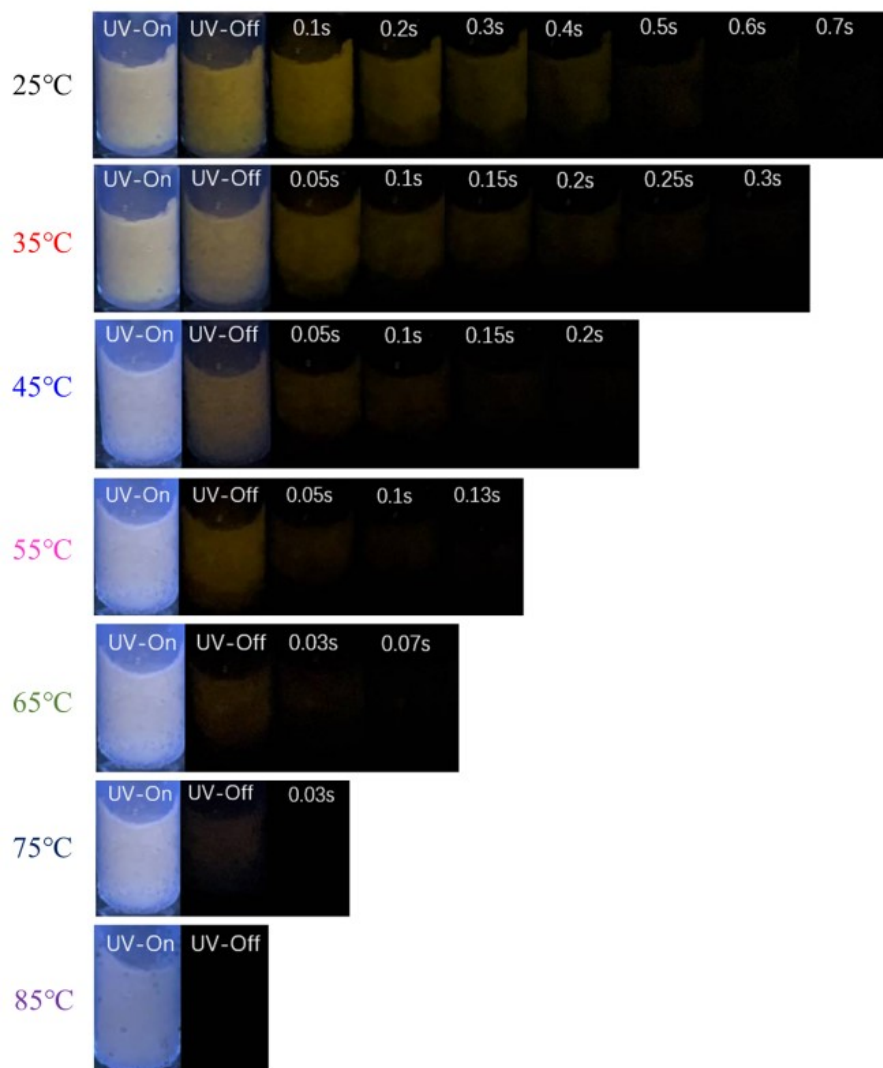


**Fig. S23** Afterglow images of **DBF-dPh** gel ( $20 \text{ mg mL}^{-1}$ ) at various temperatures.

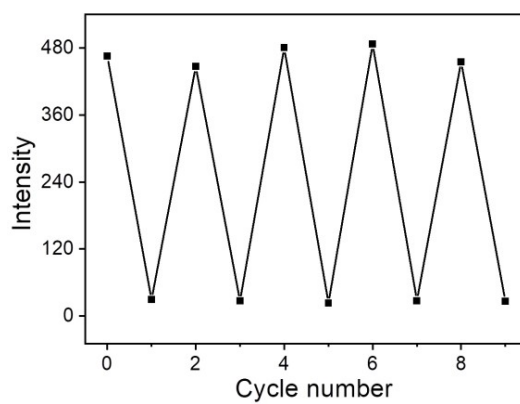


**Fig. S24** Phosphorescence switching cycles of **DBF-dPh** gel under alternating heating and cooling (Phosphorescence intensity recorded at 570 nm)



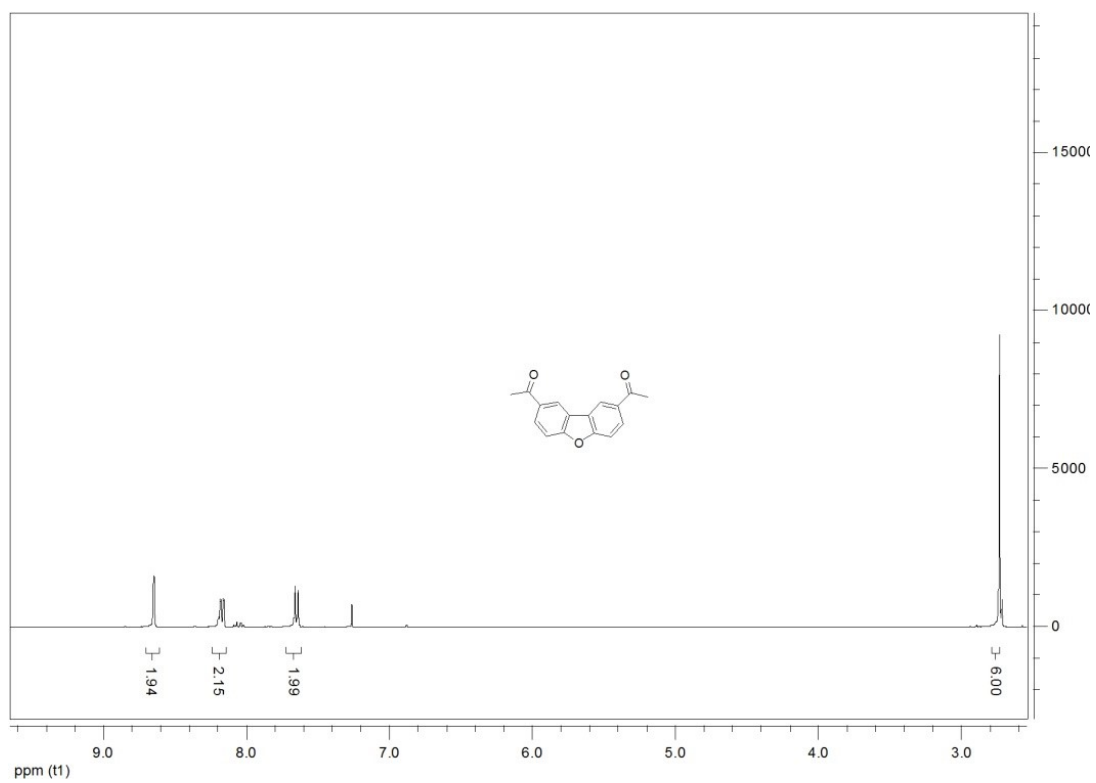


**Fig. S25** <sup>1</sup>H NMR of DBF-dAc.

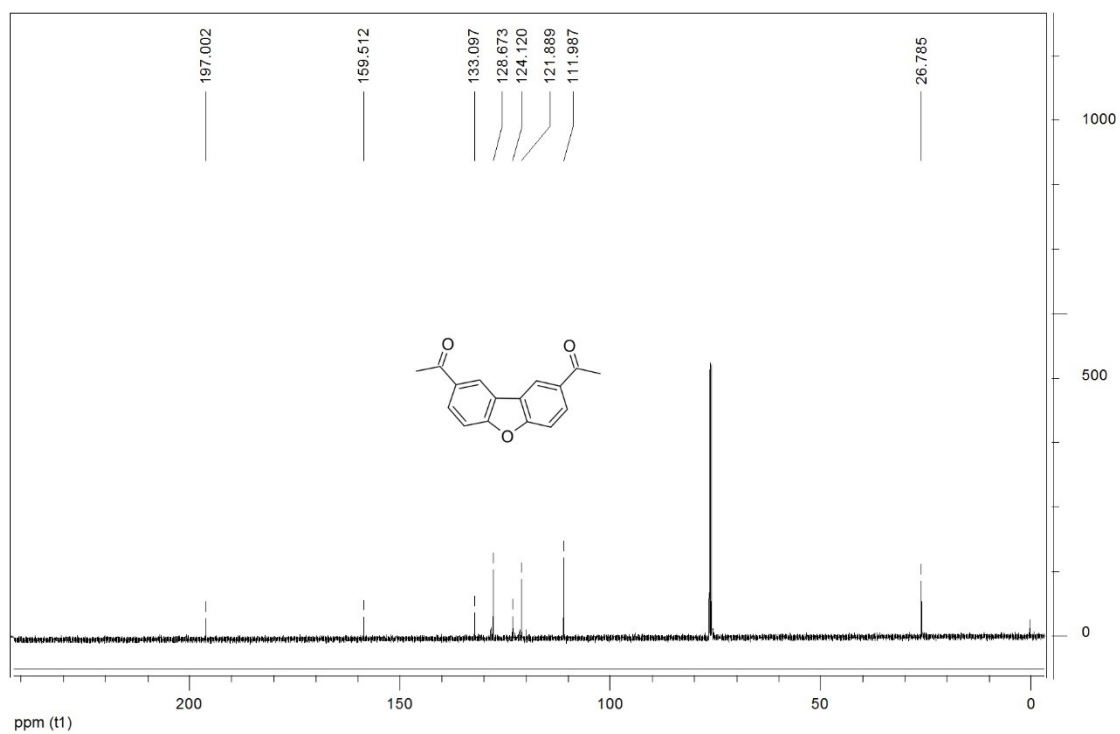


**Fig. S26** <sup>13</sup>C NMR of DBF-dAc.

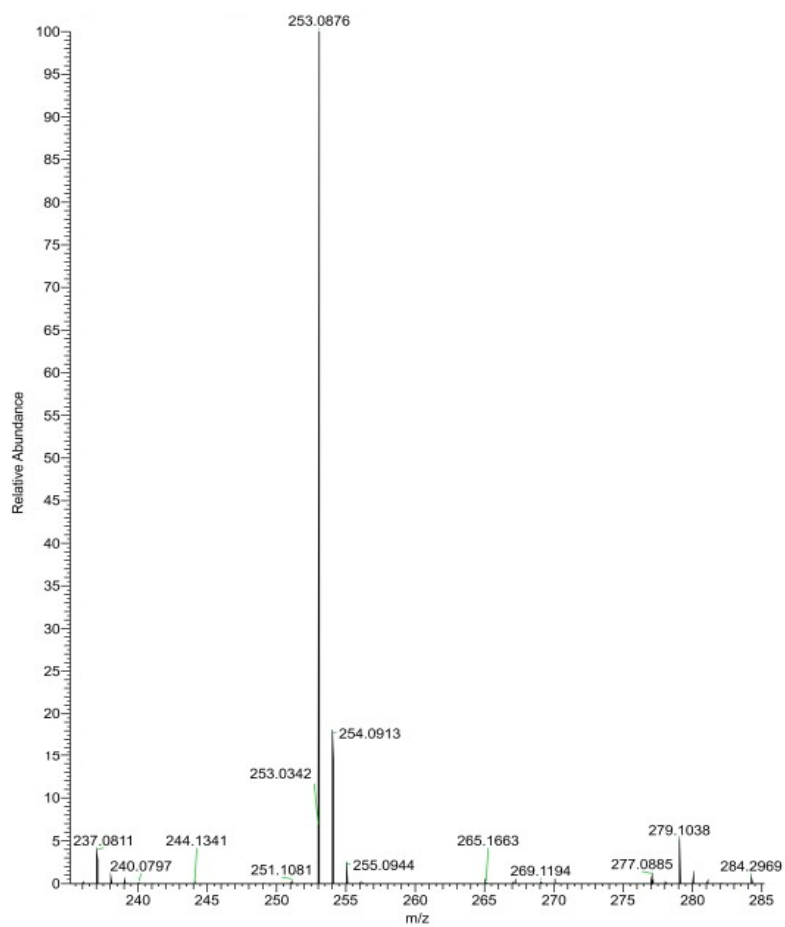


**Fig. S27** HRMS of DBF-dAc.

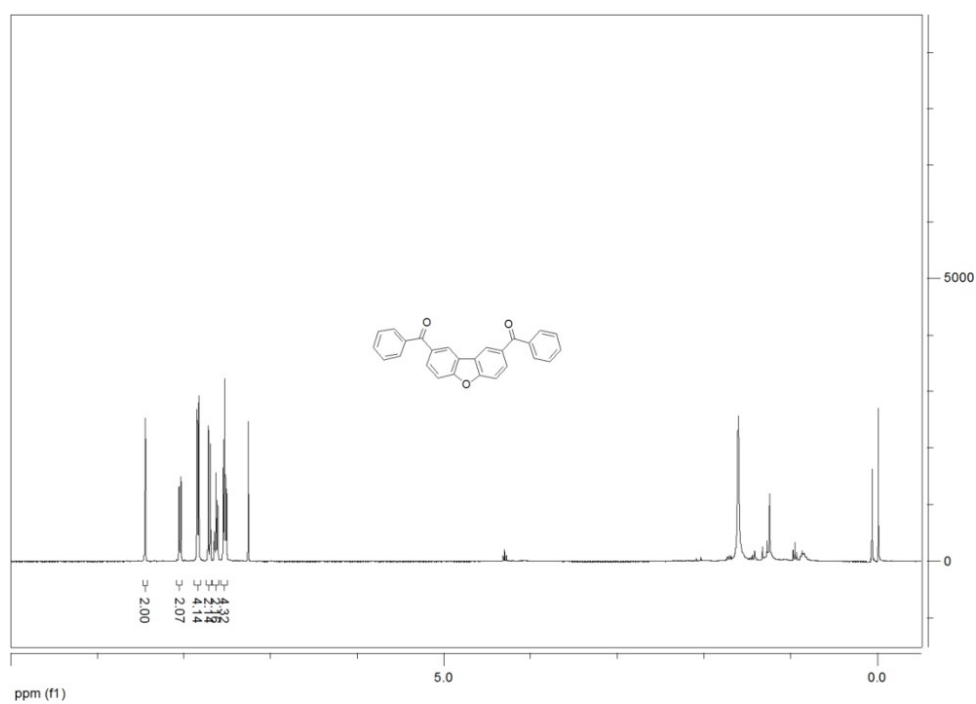


**Fig. S28** <sup>1</sup>H NMR of DBF-dPh.

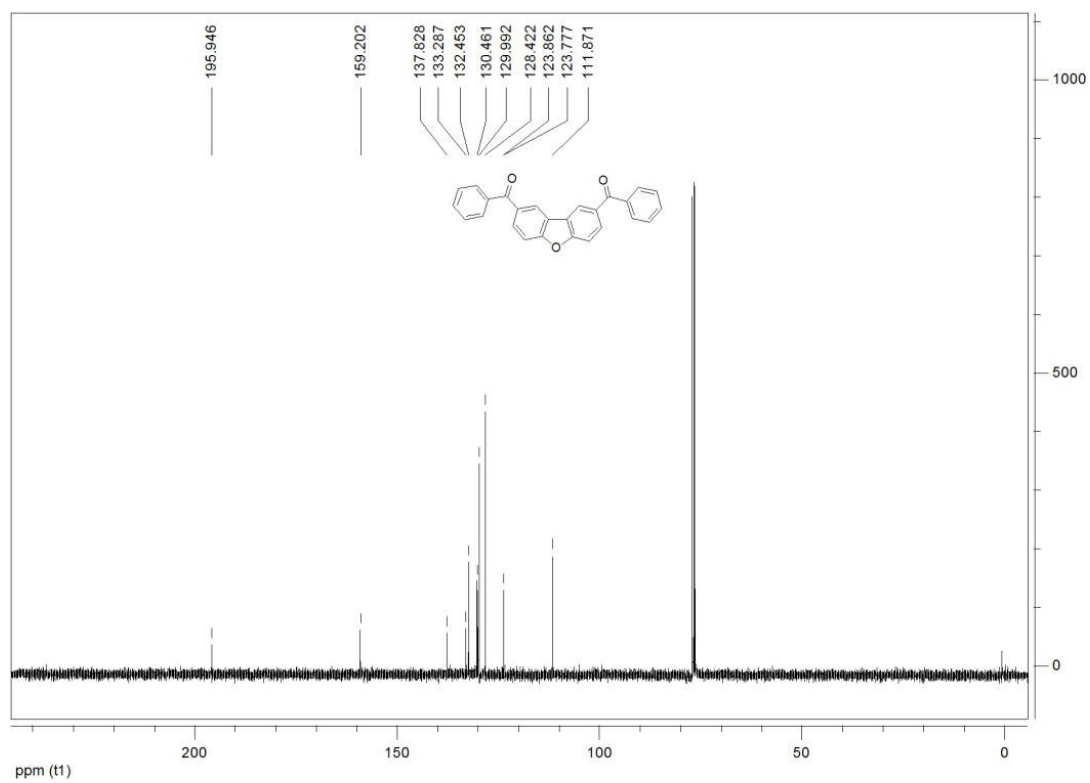


**Fig. S29**  $^{13}\text{C}$  NMR of of DBF-dPh.

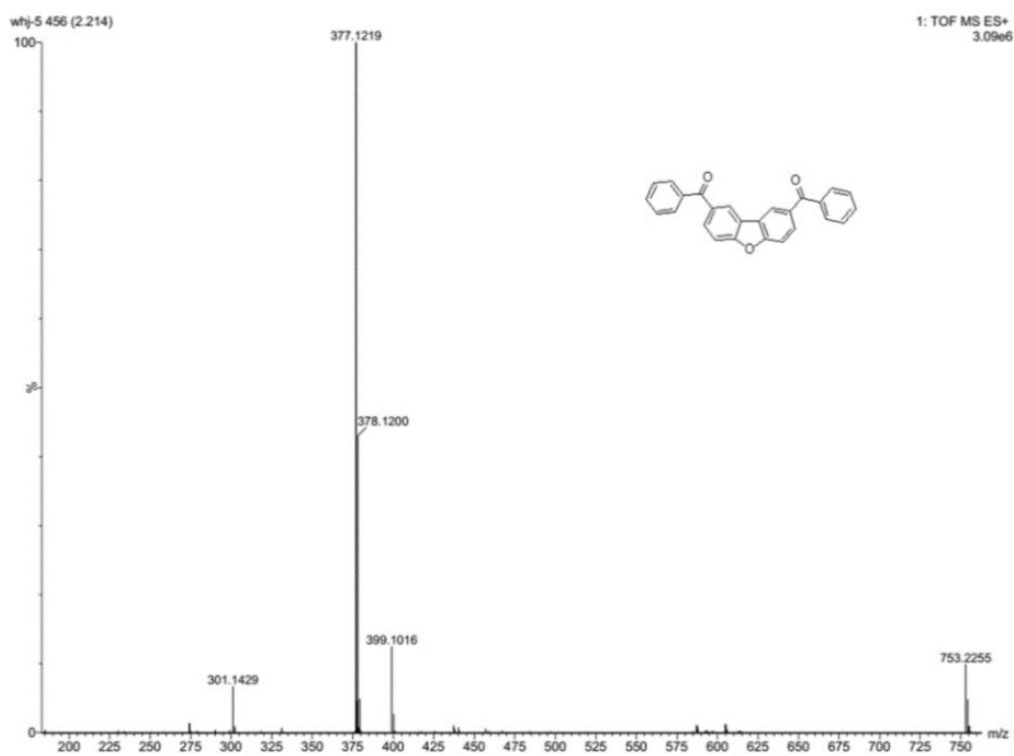


**Fig. S30** HRMS of DBF-dPh.

#### 4. References:

- 1 B. Hess, C. Kutzner, DVD. Spoel, E. Lindahl, GROMACS 4: algorithms for highly efficient, load-balanced, and scalable molecular simulation, *J. Chem .Theory Comput.*, 2008, 4, 435
- 2 R. Van Lommel, J. Y. Zhao, W. M. De Borggraeve, F. De Proft, M. Alonso, Molecular dynamics based descriptors for predicting supramolecular gelation, *Chem. Sci.*, 2020, 11, 4226.
- 3 F. Neese, Software update: the ORCA program system, version 4.0, *Wiley Interdiscip Rev. Comput Mol. Sci.*, 2018, 8, e1327.
- 4 T. Lu, F. W. Chen, Multiwfn: A multifunctional wavefunction analyzer, *J Comput Chem.*, 2012, 33, 580
- 5 S. D. Dreher, D. J. Weix, T. J. Katz, Easy synthesis of functionalized hetero [7] helicenes, *J. Org. Chem.*, 1999, 64, 3671.